Solvent Effects on the Surface Composition of Poly(dimethylsiloxane)-*co*-Polystyrene/Polystyrene Blends

Jiaxing Chen and Joseph A. Gardella, Jr.*

Department of Chemistry, SUNY at Buffalo, Buffalo, New York 14260-3000

Received April 22, 1998; Revised Manuscript Received September 29, 1998

ABSTRACT: The effects of mixed solvents used for casting films of diblock copolymer/homopolymer blends of poly(dimethylsiloxane)-*co*-polystyrene/polystyrene have been studied in detail at the surface of the films. The surface composition was determined over a wide range of detection depths using data from various spectroscopic techniques, including X-ray photoelectron spectroscopy (XPS), attenuated total reflection (ATR) FTIR, and time-of-flight secondary ion mass spectrometry (ToF SIMS). After surveying a range of solvents, the surface segregation dependence on the solvent composition was investigated for two binary solvent mixtures, namely, toluene/chloroform and cyclohexanone/chloroform. One hundred percent surface poly(dimethylsiloxane) (PDMS) coverage has been observed for the polymer blends containing 2% PDMS in bulk using the optimized cyclohexanone/chloroform mixture as solvent. Detectable amounts of polystyrene (PS) residue can be observed on surfaces for samples cast from other solvents. The PDMS-enriched surface region is much thicker for samples cast from cyclohexanone/chloroform solvent mixtures. ToF SIMS analysis results suggest that casting solvents also alter the surface morphology of sample films. The effects of solvent on the surface composition, depth gradient, and surface molecular structure of solution-cast films are discussed in terms of the polymer−solvent interaction parameters and polarity of solvents.

Introduction

The surface properties of poly(dimethylsiloxane) (PDMS) containing polymer blends have been investigated over the last 30 years since the first polymer surface modification using siloxane containing copolymers reported by Zisman and co-workers.[1] A key property of PDMS is its low surface energy, which results in surface segregation of PDMS in most polymer blend systems. This property is often desirable for many applications regarding low surface energy such as antifouling coatings.[2−4] Modification for low-energy surfaces can be achieved by blending only a small amount of PDMS containing copolymers into the homopolymer. During solidification of the material, PDMS migrates to the surface of the material, which leaves the bulk-phase properties of the material essentially unchanged. The surface properties of modified polymers prepared via surface segregation of PDMS copolymers have been shown to be directly influenced by the structure, molecular weight, and architecture of the copolymer.

The surface segregation of PDMS containing copolymers and copolymer blends has been extensively studied by our group[5−11] and many others.[3,12−15] Using contact angle measurements[13] and surface tension measurements,[14,15] various groups have reported that as little as 1% PDMS content in the polymer blends could result in almost complete PDMS surface coverage. However, recent investigations, using higher surface-sensitive and later quantitative characterization technologies such as XPS, have shown that at 1% bulk concentration, the surface is not covered completely with PDMS. A significant amount of homopolymer residue can be detected on the sample surfaces.[5,16] Special sample-processing techniques have to be used to enhance surface segregation to increase the surface coverage of PDMS.[8,17] Post-solution-cast annealing of sample films above the glass transition temperature of the polymer could enhance surface segregation to a certain extent in some blend systems.[8,9] However, annealing is not practically applicable in all circumstances. For example, degradation of the polymer may occur at elevated temperatures or the physical dimensions of the object being coated may be too large to be annealed. We have observed in our previous work[10,16−19] that the casting solvent in sample preparation significantly affects the surface segregation. Polymer−solvent interaction properties and solvent evaporation rates have been found to be factors that influence this process, but complete PDMS-covered surfaces have not been observed for low PDMS content polymer blends using a pure solvent in sample film preparation.[5,16,19] In the present study, binary solvent mixtures were investigated for casting solvent effects on the surface segregation of PDMS polymer blends. Solvent systems were selected based on our previous studies;[16] in particular, cyclohexanone/chloroform and toluene/chloroform mixtures were investigated. The surface composition of PDMS-*co*-PS/PS diblock copolymer/homopolymer blends has been studied at a wide range of sampling depths using ToF SIMS, XPS, and ATR FTIR.

Experimental Section

Materials and Sample Preparation. Diblock copolymer poly(dimethylsiloxane)-*co*-polystyrene (PDMS-*co*-PS) was provided as a donation by Dr. Dale Meier of Michigan Molecular Institute, Midland, MI. The number-average molecular weights of PDMS-*co*-PS are 70 000 for the PS block and 99 000 for the PDMS block, respectively. A standard reagent of trimethylsilyl-terminated polystyrene with a narrow molecular weight distribution was purchased from Scientific Polymer Products, Inc. Polystyrene (M_n = 280 000) was purchased from Aldrich (Milwaukee, WI). Reagent-grade solvents were used in this study; in particular, chloroform was purchased from EM Science (Gibbstown, NJ), and toluene and cyclohexanone (HPLC grade) were purchased from Aldrich. All polymers and

* To whom correspondence should be addressed.

10.1021/ma980639b CCC: $15.00
Published on Web 12/04/1998

Table 1. SolventComposition

solvent	chloroform, % by vol	second component
0	100	
		toluene
1	95	5
2	90	10
3	80	20
4	70	30
		cyclohexanone
5	98	2
6	95	5
7	93	7
8	90	10

solvents were used as received. Binary solvents were mixed by volume percentage (Table 1). Polymer sample films were solution-cast in aluminum weighing pans from 1% (w/v) solutions of each solvent composition. The cast films were allowed to air-dry at room temperature and stored in vacuum before analysis for removing solvent residue. The thickness of the sample films was controlled to about 50 μm.

XPS Analysis. All survey and high-resolution angle-dependent XPS spectra were recorded with a Perkin-Elmer 5300 XPS spectrometer with a hemispherical analyzer and a single-channel detector. Mg $K\alpha_{1,2}$ X-rays were used as the X-ray source, operated at 300 W (15.0 kV and 20 mA). The base pressure in the main chamber was maintained no higher than 5.0×10^{-8} Torr. A survey spectrum from 0 to 1000 eV was recorded for each sample film prior to high-resolution spectral acquisition. All survey spectra were recorded at a rate of 1.0 eV/step with a takeoff angle of 45° and pass energy of 89.45 eV. High-resolution spectra were acquired using the angle-dependent mode for obtaining surface composition information at different depths. Five takeoff angles were used, in particular, 10°, 15°, 30°, 45°, and 90° corresponding to detection depths of 18, 27, 52, 73, and 103 Å, respectively.[5] A pass energy of 35.75 eV and a scan energy resolution of 0.20 eV/step were used for all high-resolution XPS spectra acquisitions with a 20 eV scanning range. No radiation damage was observed during twice the time of an XPS spectrum acquisition, as evidenced from no change in the XPS spectra and no discoloration observed. At least three high-resolution acquisitions were performed for each sample.

ToF SIMS Analysis. Positive secondary ion mass spectrometry spectra were acquired on a Physical Electronics 7200 time-of-flight secondary ion mass spectrometer (ToF SIMS) equipped with a cesium ion gun and a multichannel detector. The primary ion gun was operated at 8 keV in all spectral acquisitions. The static mode was used in all acquisitions with primary ion current of 0.3 pA. The total ion dosage in each spectral acquisition was no more than 1×10^{11} ions/cm^2. A neutralizer was operated in all spectral acquisition in the pulse mode at low electron energy with a target current under 1 μA for charge compensation. Data reduction was performed using Physical Electronics TOFPak software (Version 2.0). Relative peak intensities were obtained by converting the spectra to the ASCII file format and integrating the peak area using the data analysis function built-in in Origin (Microcal Software, Inc, Northampton, MA).

ATR FTIR Analysis. All ATR FTIR spectra were recorded on a Nicolet Magna 550 FTIR spectrometer, using a resolution of 4 cm^{-1}, purged with nitrogen to ensure a stable and identical data collection environment. Five hundred scans were performed for each spectrum in all ATR FTIR acquisitions. A Harrick Scientific variable-angle multireflection ATR accessory (Model X) and germanium prisms (refractive index 4.0) were used. Taking the effective thickness as the detection depth in ATR FTIR analysis,[20,21] a detection depth of 0.68 μm was estimated for an incident angle of 45°.[22] As in XPS analysis, each sample was measured at least three times.

Data Analysis of the Experimental Results. Recalibration of the XPS Si 2p Sensitivity Factor. The accuracy of the sensitivity factors used in determining the atomic percentage is crucial in XPS quantitative analysis. Incorrect sensitivity factors would result in inaccurate atomic percentages and cause larger errors in the calculation of the atomic ratios and, consequently, reduce the reliability of the XPS quantitation results. Recalibration of the sensitivity factors including carbon 1s, oxygen 1s, and silicon 2s on this particular instrument has been done in our previous work.[23] The sensitivity factor for silicon 2p was recalibrated based on our previously determined values for carbon 1s, oxygen 1s, and silicon 2s. Pure PDMS (trimethylsilyl-terminated, Polymer Scientific Laboratories) was used for the calibration of the silicon 2p sensitivity factor. Thick films of PDMS (about 5 μm) were solution-cast on silver substrate using pure chloroform as the solvent. Calibration films were cast under nitrogen protection and solvent-evaporated directly in a XPS spectrometer prechamber to eliminate possible contamination during solvent evaporation. High-resolution XPS spectra were taken on carbon 1s, oxygen 1s, silicon 2s, and silicon 2p. The atomic concentration results of XPS on carbon 1s, oxygen 1s, and silicon 2s using our previously calibrated sensitivity factors[23] agree with the stoichiometry of PDMS within ±2%. The sensitivity factor for silicon 2p was then calculated based on carbon 1s and oxygen 1s XPS data and the stoichiometry of PDMS. The sensitivity factors used in this study are 0.24, 0.65, and 0.24 for carbon 1s, oxygen 1s, and silicon 2p, respectively.

XPS Results. High-resolution spectra of carbon 1s, oxygen 1s, and silicon 2p were recorded for the quantitative XPS analysis. The atomic ratios of carbon and silicon were used in the quantitation. According to the structures of the repeating units of PS (contains eight carbon atoms in each repeating unit) and PDMS (contains two carbon atoms and one silicon atom), the surface DMS molar fraction is expressed in terms of the carbon/silicon atomic ratio as

$$X_{\mathrm{DMS}} = \frac{8}{6 + \mathrm{C/Si}} \tag{1}$$

in which C and Si are the atomic percentages of carbon and silicon from XPS measurements, respectively.[5,25] The integration of high-resolution peaks was performed using a Perkin-Elmer Model 7500 professional computer running PHI Version 2.0 ESCA software.

ATR FTIR Results. ATR FTIR analysis provides a complementary result to XPS at an extended detection depth. The accuracy of quantitation of ATR FTIR analysis depends heavily on the calibration method. Predefined stratification structures are widely used as the model system for calibration for quantitation.[34] However, because of the unknown nature of the composition depth gradient in our samples, a predefined stratification structure cannot serve as a calibration standard in the present study. A new ATR FTIR quantitation procedure suitable for polymer blend systems with unknown surface chemical composition gradient has been developed in our laboratory.[22] A brief outline of this procedure is given here.

The calibration is based on transmission calibration on standard films with known chemical composition and thickness. The recorded transmission spectra were corrected for path-length dependence according to the penetration depth[20] in ATR measurements:

$$d_{\mathrm{p}} = \frac{\lambda_{\mathrm{d}}}{2\pi\left[\sin^2\theta - \left(\frac{n_{\mathrm{r}}}{n_{\mathrm{d}}}\right)^2\right]^{1/2}} \tag{2}$$

A calibration curve was created from the transmission spectra of standard sample files (solid line in Figure 1). Also shown in Figure 1 is a calibration curve (dashed line in Figure 1) calculated based on Beer's law using the data from the two pure samples only, which indicates that the blending of the two polymers does not cause any physical or chemical interaction that influences their IR absorption properties. A calibration equation was obtained using polynomial regression (also shown in Figure 1). This calibration curve was used throughout the ATR FTIR quantitative analysis in this study.

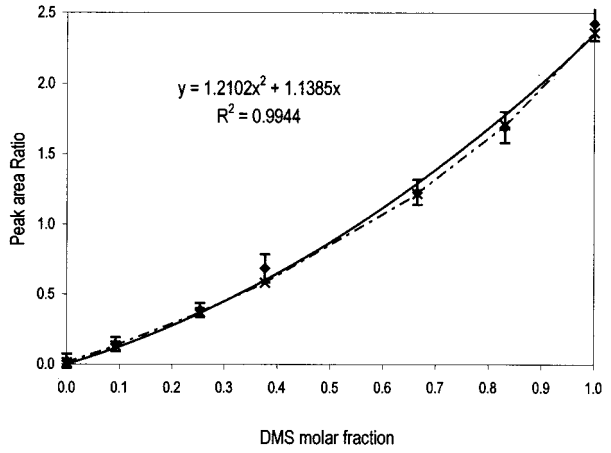

Figure 1. ATR FTIR quantification working curve from transmission calibration.

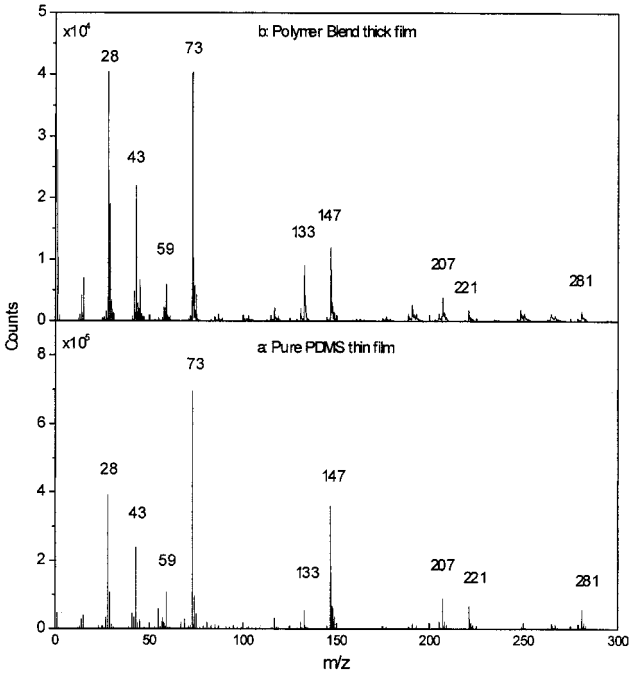

Figure 2. Low-mass portion of the positive ToF SIMS spectra of pure PDMS thin film (a) and polymer blend thick film (b).

Before peak integration on sample ATR spectra was performed, all ATR spectra were corrected for radiation penetration depth dependence of the wavelength and for physical contact quality.[20] The peak areas of selected peaks were integrated using the GRAMS/386 software (Galactic Industries Corporation, Salem, NH). The surface chemical composition was then obtained using the calibration equation.

ToF SIMS Results. Positive ToF SIMS spectra were recorded for determining the chemical composition on a much shallower surface layer, in particular, the topmost few atomic layers. The high sensitivity of ToF SIMS makes this technique an ideal method for trace analysis. Figure 2 shows the low mass portion ToF SIMS spectra of a pure PDMS film on aluminum substrate (Figure 2a) and a typical blend sample thick film (Figure 2b, about 50 μm thick free-standing film which contains 2% PDMS, cast from a binary solvent of 5% cyclohexanone in chloroform by volume). The peak at m/z = 73.048 is the most intense peak for both pure PDMS and the polymer blend sample. In the mass range below m/z = 60 in the spectra of polymer blend samples, in particular, peaks at 28 (Si^+ atomic peak), 43 (CH_3Si^+), and 59 (CH_3OSi^+) have stronger peak intensities relative to the peak at m/z = 73.048 than in the spectra of pure PDMS thin film. This is presumably due to the highly entangled molecular structure for thick films of polymer blends compared to the thin film molecular structure of pure PDMS on substrates. For the same reason, the relative intensities of higher mass peaks (m/z higher than 73) are lower for the blend sample. It should be noted that, due to stabilization effects,[26] the relative peak intensities for cyclic structure fragments (peaks of m/z 207 and higher) become stronger than the fragments from the linear structure, and this effect is more pronounced for spectra from blend samples than that from the pure PDMS. We believe this is due to the highly entangled molecular structure in thick films which requires a higher energy in forming secondary ion fragments that make fragments less stable than that from thin films.

What we wish to demonstrate is whether a complete PDMS segment layer has formed on the blend surface at the ToF SIMS detection depth. Next we wish to examine the solvent effects on surface segregation at that sampling depth. It is well-known that the dominant peak in the spectra of PS is at m/z = 91.055, due to the tropylium cation $C_7H_7^+$ rearranged from the phenyl ring of styrene.[30,31] Although it is not exclusively characteristic for PS, this peak can be used in this system to track the existence of PS on sample surfaces since PDMS does not have an aromatic ring structure. We have observed, although there is only very low intensity relative to the peak at m/z = 73.048, that the tropylium cation fragment peak does exist in all ToF SIMS spectra we collected. Thus, small amounts of PS are still detectable by ToF SIMS.

More importantly, remarkable differences on the surface composition have been observed in the spectra from films cast from different solvent mixtures. By taking the relative peak intensity of the characteristic peaks of PDMS and PS in the ToF SIMS spectra, we were also able to describe the trend in solvent effects on surface segregation on the top few atomic layers.[33]

Results and Discussion

Table 2 lists all results of the surface DMS concentration of the PDMS-*co*-PS/PS diblock copolymer/homopolymer blend films cast from different solvents by both XPS and ATR FTIR quantitative analysis. Surface PDMS concentration data are provided in the molar fraction of the DMS repeating units, followed with the standard deviation (in parentheses) to show the reproducibility of the quantitative analysis results. A discussion on the results below will highlight some of the important features.

Figure 3 shows the surface DMS concentration versus bulk DMS concentration from XPS data of 10°, 30°, and 90° takeoff angles of pure chloroform-cast films. At the shallowest sampling depth (10° takeoff angle, which corresponding to 18 Å of sampling depth), the surface DMS concentration increases quickly from 92% for 1% bulk PDMS sample to 95% for 2% bulk PDMS sample and then reaches 98% for 3% bulk PDMS sample where the surface PDMS concentration levels off. At deeper layers, the changes in the surface PDMS concentration are even more pronounced. For instance, at 103 Å, the surface PDMS concentration increases from 73% for 1% bulk PDMS sample to 85% for 2% bulk PDMS sample, indicating a thicker region of surface segregation. However, the fact that the surface PDMS concentration levels off at 3% bulk PDMS concentration indicates that further increases in bulk PDMS concentration will not significantly increase the surface PDMS concentration, although they may result in a thicker PDMS-rich region. We have previously reported[16] the extent of surface segregation of PDMS in polymer blends using different pure solvents. Although solvents used in film preparation influence the process of surface segregation significantly, we have never observed 100% surface PDMS

Table 2. Surface PDMS Concentration (in DMS M %)

		at depth[b,c]					
bulk DMS, mol %	solvent,[a] vol %	18A	27A	52A	73A	103A	700A
1.0	0.0	92.4(1.0)	89.5(1.1)	83.7(1.0)	78.9(1.0)	73.4(1.0)	9.0(5.0)
1.0	5.0	92.6(1.3)	92.4(1.0)	87.3(1.0)	82.2(1.0)	74.8(1.0)	14.0(5.0)
1.0	10.0	94.5(1.0)	91.6(1.0)	87.7(1.0)	80.9(1.0)	78.4(1.0)	14.9(5.0)
1.0	20.0	94.9(1.0)	91.6(1.0)	88.4(1.0)	86.5(1.0)	81.8(1.0)	16.6(5.0)
1.0	30.0	95.4(1.0)	92.6(1.0)	87.9(1.0)	82.2(1.0)	75.6(1.0)	16.9(5.0)
2.0	0.0	95.1(1.3)	93.7(1.0)	92.2(1.0)	89.5(1.0)	84.9(1.0)	15.1(5.0)
2.0	5.0	95.8(1.1)	95.1(1.0)	93.6(1.4)	91.4(1.0)	88.2(1.0)	20.3(5.0)
2.0	10.0	96.3(1.0)	95.8(1.0)	95.2(1.0)	92.9(1.0)	90.0(1.0)	22.6(5.0)
2.0	20.0	97.9(1.0)	97.0(1.0)	96.0(1.2)	92.5(1.4)	89.6(1.0)	26.2(5.0)
2.0	30.0	99.6(1.0)	98.0(1.1)	95.0(1.6)	90.6(1.0)	86.4(1.0)	23.8(5.0)
3.0	0.0	97.9(1.0)	97.7(1.0)	97.0(1.0)	94.5(1.0)	91.8(1.0)	20.3(5.0)
3.0	0.0	97.9(1.0)	96.7(1.0)	95.7(1.0)	93.9(1.0)	89.5(1.0)	27.4(5.0)
3.0	10.0	98.0(1.0)	97.2(1.0)	96.2(1.6)	93.9(1.0)	90.0(1.0)	29.5(5.0)
3.0	20.0	98.6(1.0)	98.2(1.0)	95.7(1.0)	92.2(1.0)	87.8(1.0)	30.8(5.0)
3.0	30.0	99.4(1.0)	98.0(1.0)	94.2(1.5)	88.7(1.0)	81.2(1.0)	31.2(5.0)
4.0	0.0	98.5(1.2)	98.2(1.0)	97.3(1.0)	95.1(1.0)	91.9(1.0)	33.4(5.0)
4.0	5.0	98.6(1.0)	98.2(1.0)	96.8(1.0)	94.3(1.0)	91.1(1.0)	33.8(5.0)
4.0	10.0	98.1(1.0)	97.1(1.0)	95.3(1.1)	94.0(1.0)	89.5(1.4)	35.2(5.0)
4.0	20.0	97.5(1.4)	94.8(1.0)	92.5(1.0)	89.2(1.2)	84.1(1.0)	40.0(5.0)
4.0	30.0	97.6(1.2)	96.7(1.0)	95.2(1.0)	92.5(1.0)	88.6(1.0)	43.5(5.0)
1.0	0.0	92.4(1.0)	89.5(1.1)	83.7(1.0)	78.9(1.0)	73.4(1.0)	9.0(5.0)
1.0	2.0	96.4(1.0)	97.2(1.0)	93.8(1.0)	93.5(1.0)	83.5(1.0)	23.2(5.0)
1.0	5.0	98.0(1.0)	97.2(1.0)	95.3(1.0)	91.5(1.0)	87.9(1.0)	28.7(5.0)
1.0	7.0	96.8(1.0)	96.2(1.0)	94.9(1.0)	89.0(1.0)	86.0(1.0)	32.1(5.0)
1.0	10.0	96.6(1.1)	96.2(1.0)	93.0(1.0)	92.4(1.0)	82.9(1.0)	29.2(5.0)
2.0	0.0	95.1(1.3)	93.7(1.0)	92.2(1.0)	89.5(1.0)	84.9(1.0)	15.1(5.0)
2.0	2.0	99.4(1.0)	98.5(1.0)	95.8(1.0)	92.4(1.0)	88.0(1.4)	24.0(5.0)
2.0	5.0	100.3(1.0)	100.0(1.0)	98.4(1.0)	97.0(1.0)	94.5(1.0)	30.1(5.0)
2.0	7.0	100.2(1.0)	100.0(1.0)	99.0(1.0)	97.7(1.0)	94.6(1.1)	33.7(5.0)
2.0	10.0	98.8(1.0)	96.5(1.0)	92.6(1.0)	89.0(1.0)	85.3(1.0)	31.7(5.0)
3.0	0.0	97.9(1.0)	97.7(1.0)	97.0(1.0)	94.5(1.0)	91.8(1.0)	20.3(5.0)
3.0	2.0	99.1(1.3)	99.4(1.3)	98.2(1.0)	95.4(1.0)	91.8(1.0)	28.2(5.0)
3.0	5.0	100.1(1.1)	99.4(1.0)	98.8(1.0)	97.1(1.0)	94.9(1.0)	38.4(5.0)
3.0	7.0	99.7(1.0)	98.6(1.5)	97.6(1.0)	96.2(1.0)	93.1(1.0)	39.8(5.0)
3.0	10.0	98.6(1.0)	98.4(1.0)	96.9(1.0)	95.9(1.0)	91.8(1.0)	38.5(5.0)
4.0	0.0	98.5(1.0)	98.2(1.0)	97.3(1.0)	95.1(1.0)	91.9(1.0)	33.4(5.0)
4.0	2.0	98.8(1.0)	98.8(1.0)	98.0(1.0)	96.6(1.0)	94.1(1.3)	41.3(5.0)
4.0	5.0	99.4(1.4)	98.3(1.2)	98.2(1.0)	97.6(1.1)	95.8(1.0)	43.9(5.0)
4.0	7.0	97.8(1.3)	98.1(1.2)	98.2(1.0)	97.7(1.0)	94.5(1.0)	46.6(5.0)
4.0	10.0	97.2(1.2)	97.0(1.4)	95.3(1.0)	92.9(1.0)	88.9(1.0)	46.6(5.0)

[a] Binary solvent mixed with chloroform. Solvent is toluene in top half of table and cylohexanone in the bottom half. [b] XPS results except the last column, which is ATR FTIR results. [c] In parenthesis is ± standard deviation.

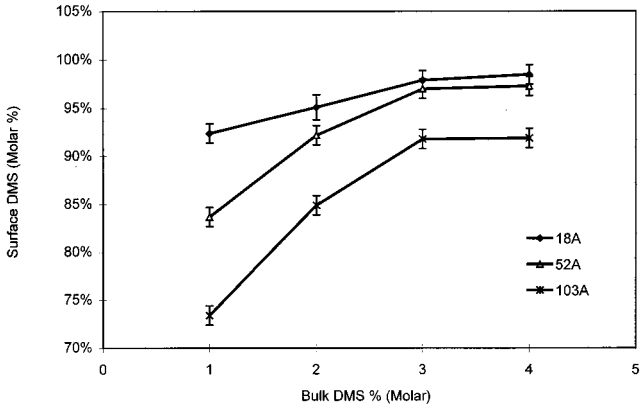

Figure 3. Surface DMS versus bulk DPS concentration by XPS at different detection depths. Sample films cast from pure chloroform.

concentration for low bulk PDMS concentration (<3%) in PS blends.

Influence of Polymer−Solvent Interaction on Surface Segregation. In considering the mixing thermodynamics of polymers with solvents, PDMS has an opposite interaction characteristic with many common solvents compared with PS. This behavior can be explained using polymer−solvent interaction parameters[27] (χ). For example, when the χ parameter is plotted versus the polymer volume fraction in solution, PDMS shows an increasing trend in toluene as the concentration of the solution increases, while PS shows a declining trend. This suggests that during solvent evaporation, the mobility of the PDMS segments will decrease faster than in PS due to the solvation of polymer segments in solution. However, the χ parameter of PDMS in chloroform is essentially unchanged, while the polymer volume fraction increases from 0 to 1 (Figure 4). It can be expected that, if a poor solvent for PDMS is mixed with chloroform, the decrease in mobility of the PDMS segments makes the cohesive migration of PS segments more efficient, therefore encouraging preferential precipitation of PDMS segments and resulting in higher surface segregation, while PS segments still retain high mobility. This is exemplified by samples cast from chloroform/toluene mixtures. Figure 5 shows the surface PDMS concentration dependence of the toluene concentration in binary solvent mixtures. At the XPS-detected topmost layer, the surface PDMS concentration increased from 92% (cast from pure chloroform) to 95% (cast from both 20% and 30% toluene mixtures) for samples with 1% bulk PDMS concentration. For 2% bulk PDMS concentration samples, the surface PDMS concentration increased from 95% (cast

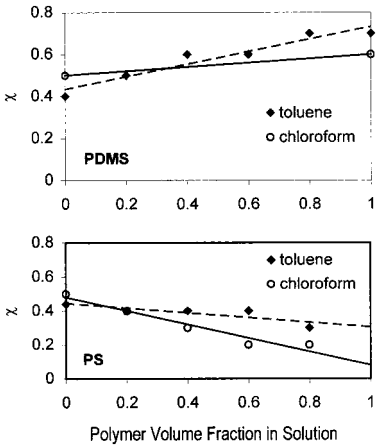

Figure 4. Polymer−solvent interaction parameter χ versus polymer molar fraction. Data taken from ref 27.

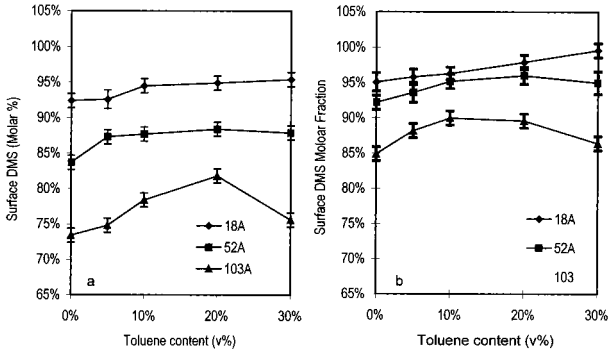

Figure 5. Surface DMS versus toluene concentration by XPS. a, 1% bulk DMS content; b, 2% bulk DMS content.

from pure chloroform) to virtually 100% (cast from 30% toluene mixture). The results show that the surface DMS concentration varies substantially depending on the solvent composition.

Solvent Polarity Effects on Surface Segregation. It has been observed in previous studies that solvents with higher boiling points could increase the surface segregation, presumably due to the prolonged solvent evaporation time. For example, when sample films of BPAC−PDMS copolymer were cast by pyridine or ethylene chloride, at the shallowest surface, the PDMS concentration of the as-cast films by pyridine is slightly higher than that cast by ethylene chloride, but not statistically significant.[24] What was noticeable was the difference in depth gradient of PDMS and the change of PDMS concentration upon annealing treatments. For films cast from pyridine, annealing did not make a detectable increase in the surface DMS concentration or a change in the depth distribution. In contrast, annealing methylene chloride cast films increased the surface DMS by 4% or more at all depths. This phenomenon was understood as the lower solvent evaporation rate of pyridine provides a longer time for polymer segments to move toward thermodynamic equilibrium before the polymer matrix solidifies. In the present study, up to 10% cyclohexanone was mixed with chloroform to form binary solvents. Figure 6 shows the solvent dependence of the surface DMS concentration for 1% bulk PDMS content samples (Figure 6a) and 2% bulk PDMS content samples (Figure 6b), respectively. The graphs show that the surface PDMS concentration first increases as the concentration of cyclohexanone increases and then peaks and declines. This phenomenon cannot be interpreted simply as the extension of solvent evaporation time.

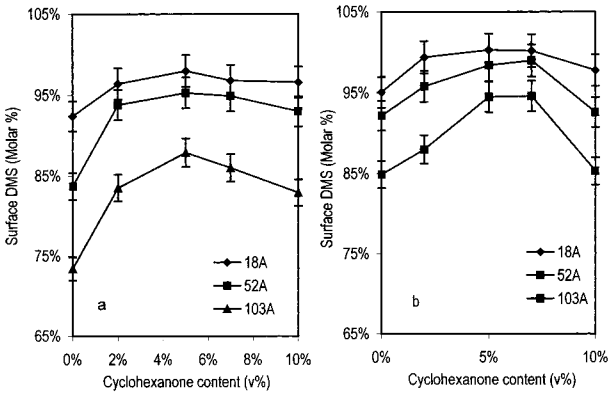

Figure 6. Surface DMS versus cyclohexanone concentration by XPS. a, 1% bulk DMS content; b, 2% bulk DMS content.

Table 3. Solubility Parameters of Solvents[a]

solvent	Hansen params	δ_d	δ_p	δ_h	Hildebrand params
chloroform	19	17.8	3.1	5.7	19
toluene	18.2	18	1.4	2	18.2
cyclohexanone	19.6	17.8	6.3	5.1	20.3

[a] Data adopted from ref 27.

By considering the polarity of the solvent, the surface segregation behavior of PDMS in this solvent can be understood. For example, the polarity term in the Hansen parameters[27] for chloroform is 3.1, while that for cyclohexanone is 6.3 (Table 3). There is a strong local polarity for PDMS along the silicon−oxygen bond due to the difference in electronegativity of the two elements (gas-phase dipole moment of OSi = 3.1 D[32]). Compared with PDMS, the local polarity in polystyrene is much weaker (local polarity in PS is along the axis of the aromatic ring structure, which has a gas-phase dipole moment of 0.38 D[32]). When cyclohexanone is mixed with chloroform in small portions, the solvation of cyclohexanone molecules would selectively occur around PDMS segments. The better solvated PDMS segments help the surface segregation of PDMS and cohesive migration of PS toward the bulk more efficiently. It is interesting to note that for lower bulk PDMS content samples (1% bulk PDMS), the surface PDMS concentration peaks at lower cyclohexanone concentrations than samples with higher bulk PDMS concentrations. This suggests that selective solvation of PDMS segments by cyclohexanone is the key issue. It could be predicted that when an excess amount of cyclohexanone exists in the solvent, the solvation of PS segments by cyclohexanone molecules is also increased, which makes the surface segregation of PDMS less efficient.

Different from the toluene/chloroform binary solvents, which enhance surface segregation through selective precipitation, cyclohexanone promotes surface segregation by selective solvation of PDMS segments, and thus, the surface segregation would be expected to extend to deeper layers. Figures 7 and 8 show surface PDMS concentrations of 1% and 2% bulk PDMS content sample at greater depths by ATR FTIR measurements. The fact that the surface PDMS concentrations of the cyclohexanone mixture cast samples are about 8% higher than for samples cast from toluene mixtures at this detection depth indicates the active segregation region is much broader than that in the former case. Furthermore,

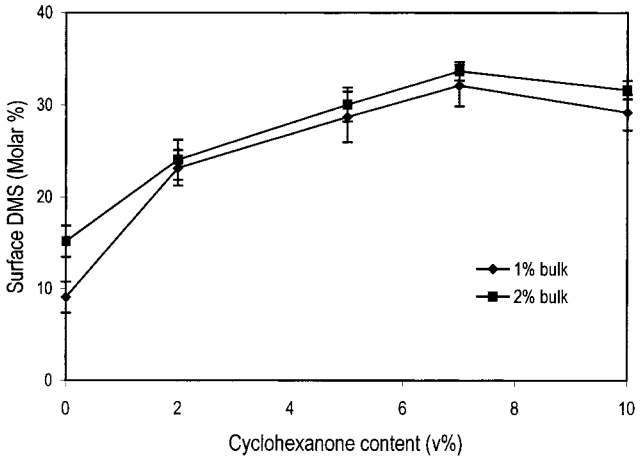

Figure 7. Surface DMS versus cyclohexanone concentration in solvent by ATR FTIR at detection depth of 0.7 μm.

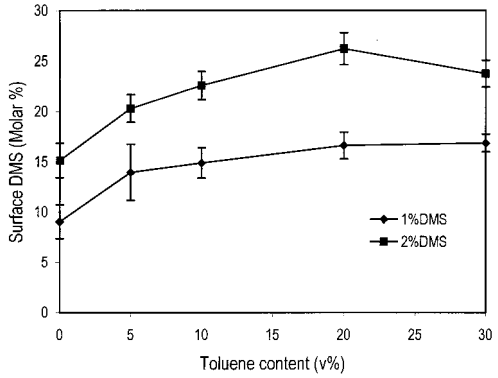

Figure 8. Surface DMS versus toluene concentration in solvent by ATR FTIR at detection depth of 0.7 μm.

there is no significant difference in the surface PDMS concentrations between 1% and 2% bulk PDMS content in cyclohexanone/chloroform cast samples, while the difference in the toluene mixture cast sample is very pronounced. This also serves as evidence that the active surface segregation region in cyclohexanone/chloroform cast films is thicker than films cast from the toluene mixtures.

Depth Profile. The difference in mechanisms of promoting surface segregation by solvents can also be seen by considering the in-depth profile of the PDMS concentration produced by combining the results from different methods. For toluene-containing solvent mixtures, the increase in the free energy of mixing toward the increase of the polymer volume fraction of PDMS (Figure 4) indicates that a preferential precipitation of PDMS segments may occur during solvent evaporation. This limits surface segregation to a narrower range in depth from the surface. In contrast, the existence of cyclohexanone in the solvent increases the degree of solvation around the PDMS segments; therefore, polymer segments could keep significant mobility even when very little solvent is left in the polymer. This is exemplified by Figure 9, a plot of detected PDMS concentrations versus depths over a wide sampling range by XPS and ATR FTIR. Throughout the broad depth range, PDMS concentration detected on the surface is higher for films cast from cyclohexanone mixtures than those cast from toluene binary solvent without an exception. At deeper layers detected by ATR FTIR, the difference in the PDMS concentration appears to be even greater than at the shallower layers measured by XPS.

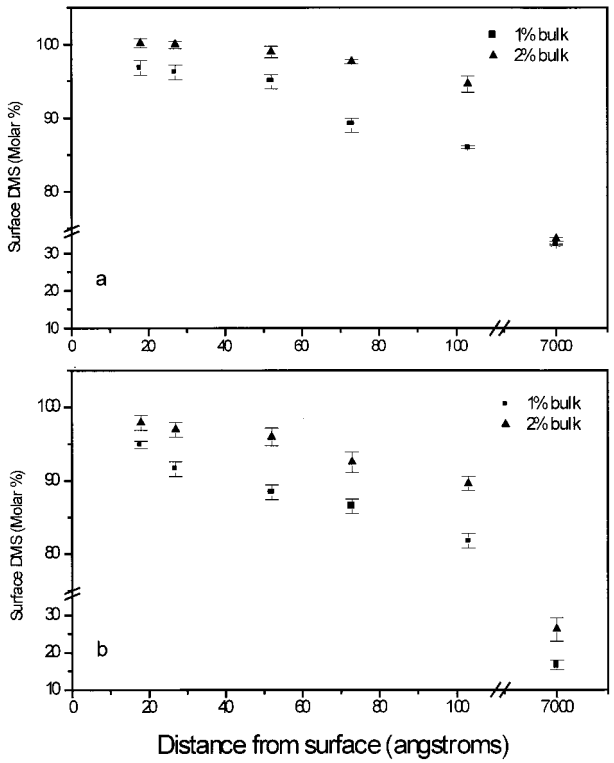

Figure 9. Surface DMS depth gradient by XPS and ATR FTIR. a, cast from 7% cyclohexanone in chloroform; b, cast from 20% toluene in chloroform.

Table 4. Relative Surface PS Concentration

casting solvent	A73/A91[b]	concn[a]
pure chloroform	47(3)	1
20% toluene in chloroform	137(8)	0.34
7% cyclohexanone in chloroform	562(34)	0.08

[a] Figures show the relative values of surface PS concentration when taking the surface PS concentration of pure chloroform casting films as the unit. [b] Numbers in parentheses are the standard deviation.

Surface Composition by ToF SIMS Analysis. Although 100% PDMS has been observed on sample surfaces using XPS, we cannot rule out the possibility that trace amounts of PS residue remain on the surface due to the relatively low sensitivity of XPS as compared with ToF SIMS. Taking the advantage of the parts per million sensitivity of ToF SIMS, we not only detected very small amounts of PS residue on the top few atomic layers of the surface but also clearly observed the solvent effects on surface segregation by measuring the relative peak intensities of the trimethylsilyl cation (m/z = 73.048) and the tropylium cation (m/z = 91.055). The relative peak intensities from samples all containing 2% PDMS in the bulk and cast from different solvents are listed in Table 4. The surface PS concentration differences due to casting solvents can be quantitatively evaluated as the ratio of relative peak intensities as shown in Table 4. These results are consistent with that from XPS and ATR FTIR quantitation. Figure 10 shows ToF SIMS images of surface PDMS and PS represented by fragments of trimethylsilyl cations and tropylium cations. Data illustrated by the images show that the distribution of PS residues is also different. Larger microdomains may exist on the surfaces of the pure chloroform-cast films, while binary-solvent-cast films have much smaller microdomains of PS.

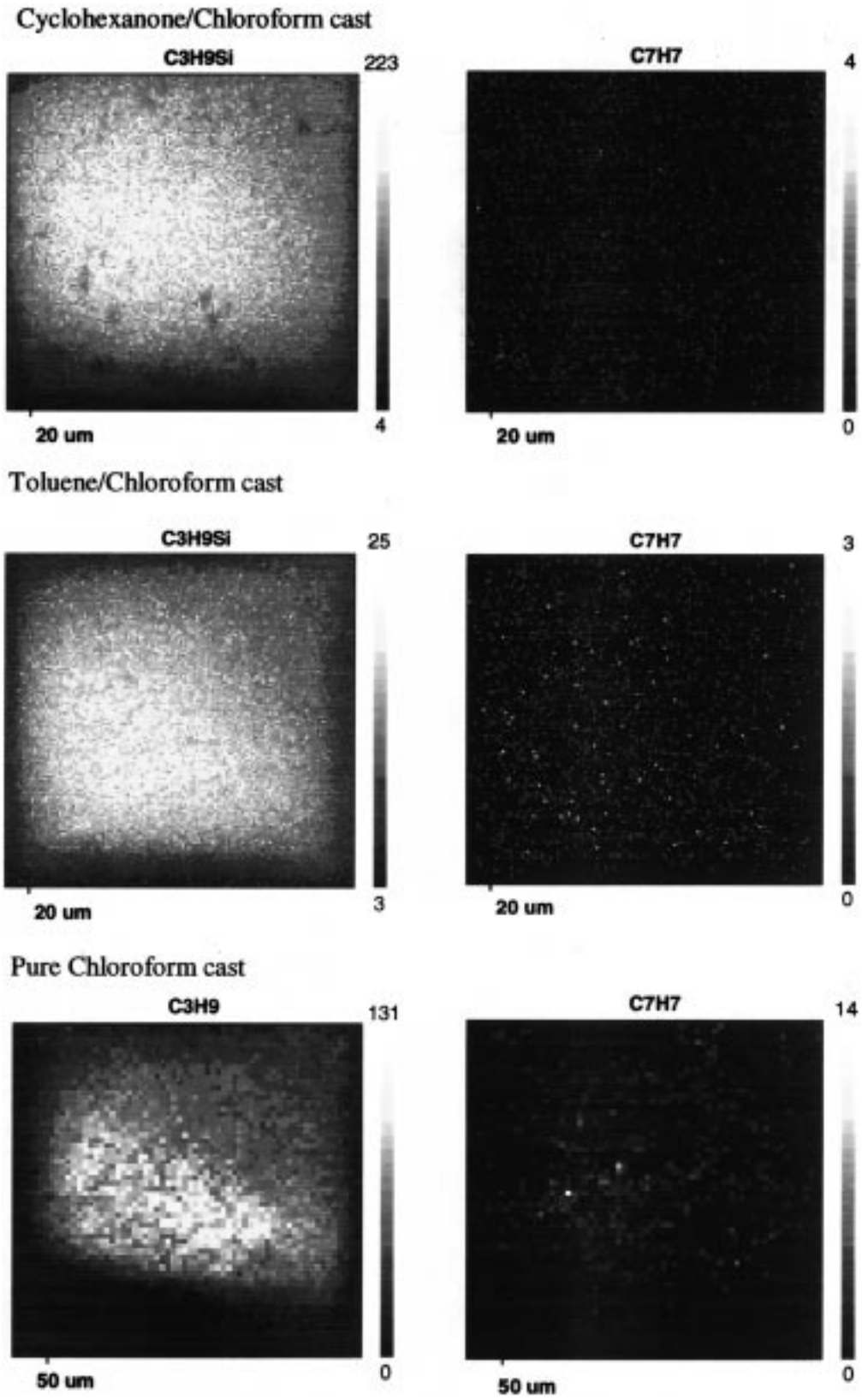

Figure 10. ToF SIMS image of samples cast from different solvents.

End-Group Preferential Orientation. Previous studies of PDMS by both mass spectrometry[28] and SIMS[29] suggested that the trimethylsilyl fragment ($Si(CH_3)_3^+$) results from rearrangements of the PDMS backbone chain fragments. However, a more recent study on PDMS[30] and then poly(methylphenylsiloxane)[31] (PMPS) suggests the $Si(CH_3)_3^+$ fragment may come solely from the trimethylsilyl end group. In PMPS samples that are not terminated by trimethylsilyl, the $Si(CH_3)_3^+$ fragment was not detected.[31] Clarson and coworkers also attributed the high intensity of the $Si(CH_3)_3^+$ to end-group enrichment due to the low surface energy and large free volume of the trimethylsilyl group. Therefore, a comparison of the fragment peak intensities of the higher mass species among samples prepared with different methods would help to

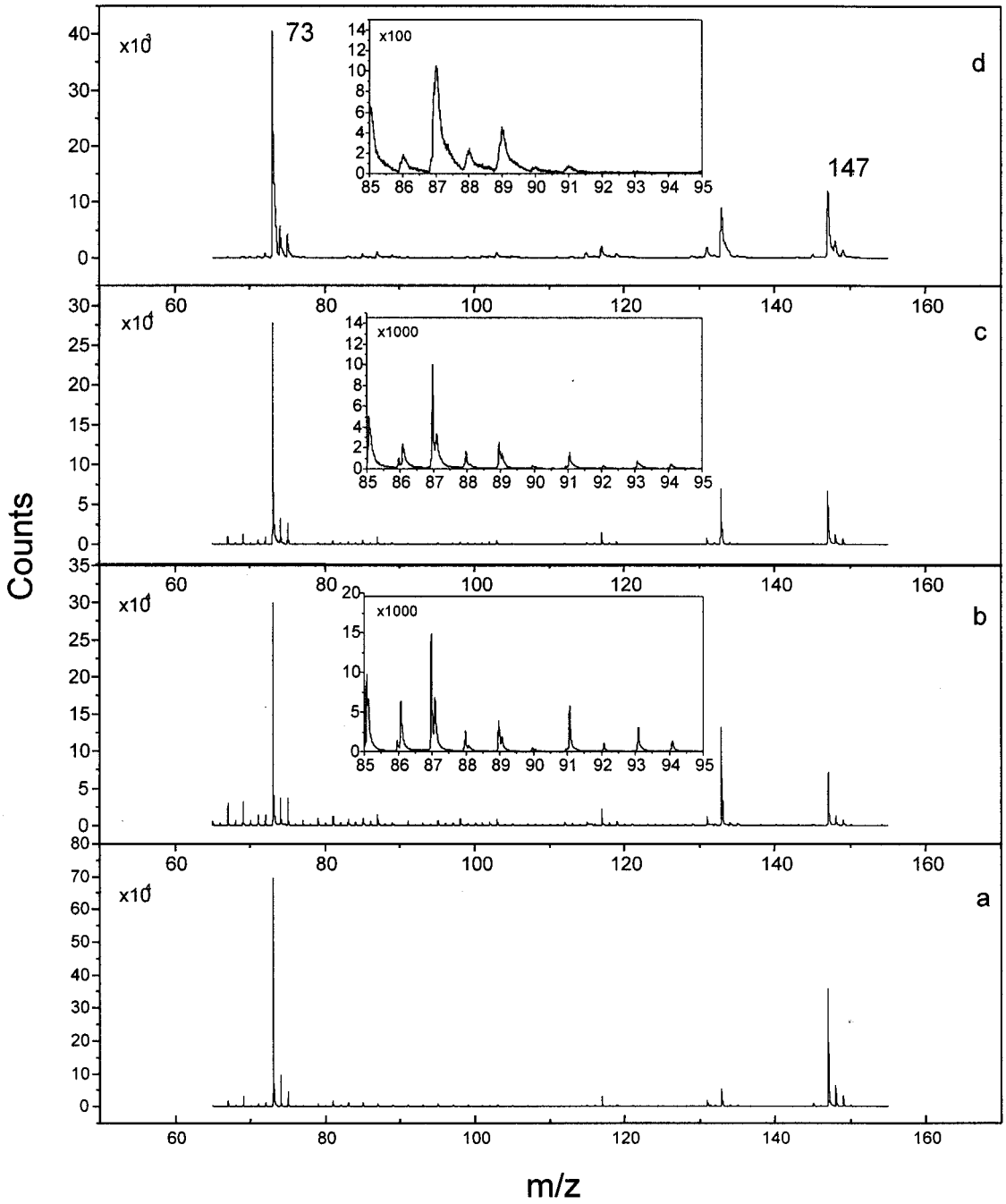

Figure 11. log plot of ToF SIMS spectra of $m/z = 60-160$. a, pure PDMS thin film on aluminum; b, polymer blend cast from pure chloroform; c, polymer blend cast from 20% toluene in chloroform; d, polymer blend cast from 7% cyclohexanone in chloroform. Samples b−d all contain 2% PDMS in bulk.

distinguish if the casting solvent affects end-group preferential orientation only or PDMS segments in the surface segregation. The $m/z = 73$, 147, and 221 fragment series in PDMS has an exponential intensity−decay pattern. The $m/z = 147$ peak is due to $Si(CH_3)_2OSi(CH_3)_3^+$, one PDMS repeating unit longer than the trimethylsilyl end group, and the peak at $m/z = 221$ is one more repeating unit longer than the $m/z = 147$ peak. Figure 11 shows the comparison of the relative intensities in this series from samples cast by different solvents. Figure 11a is the spectrum from a pure PDMS monolayer film cast on an aluminum substrate. In a monolayer, the polymer chain can be considered to be laying flat on the substrate, and the end-group preferential orientation effect at the polymer surface is eliminated. Therefore, it can be considered that the fragmentation from a monolayer film is not to be affected by end-group preferential orientation effects. Parts b, c, and d of Figure 11 are spectra of blend sample thick films of 2% bulk PDMS content, cast from pure chloroform, 20% toluene in chloroform, and 7% cyclohexanone in chloroform, respectively. Figure 11a has the highest relative intensity of peak $m/z = 147$ to $m/z = 73$, suggesting higher ion yield of longer segment fragments from flat-laying polymer molecules on the substrate. Based on this, we could assume that the higher relative intensity of these two peaks means more PDMS segments exist on the sample surface. Figure 11 suggests that the cyclohexanone binary-solvent-cast sample have the strongest relative intensity of these two peaks. It is not a surprise that the PDMS thin film on the substrate gives the highest relative intensity be-

cause of the chain entanglement in the thick polymer films. This trend holds for the higher *m*/*z* peaks in this sequence. This means that PDMS segments, not only the trimethylsilyl end group, exist at the topmost layer, and the surface structure is indeed solvent-dependent.

Conclusion

The surface composition of PDMS-*co*-PS/PS diblock−copolymer/homopolymer blends has been studied in detail over a wide range of detection depths using XPS, ATR FTIR, and ToF SIMS. Solvent effects on the surface segregation process are revealed. A complete PDMS segment layer surface coverage is achieved using a binary solvent mixture of chloroform and cyclohexanone with 2% bulk PDMS content. A further increase of the bulk PDMS concentration does not make a detectable increase in the surface PDMS concentration. For samples containing less than 2% bulk PDMS content, the surface PDMS concentration difference is detectable at different depths of measurements. ToF SIMS measurements reveal that a complete surface PDMS layer has formed via surface segregation in cyclohexanone binary-solvent-cast films. Small amounts of PS segment residue can be detected on sample surfaces by ToF SIMS for both toluene-containing binary solvent and pure chloroform-cast films.

Evidence shows through ToF SIMS spectra that the casting solvent during the sample preparation has also changed the surface morphology. The solvent effects on the surface morphology in the topmost layer need to be further investigated.

References and Notes

(1) Jarvis, N. L.; Fox, R. B.; Zisman, W. A. *Adv. Chem. Ser.* **1964**, *43*, 317.
(2) Owen, M. J. *Commun. Inorg. Chem.* **1988**, *7*, 195.
(3) Yilgor, I.; McGrath, J. E. *Adv. Polym. Sci.* **1988**, *86*, 1.
(4) Owen, M. J. In *Siloxane Polymers*; Clarson, S. J., Semlyen, J. A., Eds.; Prentice Hall: Englewood Cliffs, NJ, 1993.
(5) Chen, X.; Kumler, P. L.; Gardella, J. A., Jr. *Macromolecules* **1992**, *25*, 6621.
(6) Chen, X.; Kumler, P. L.; Gardella, J. A., Jr. *Macromolecules* **1992**, *25*, 6631.
(7) Gardella, J. A., Jr.; Ho, T.; Wynne, K. J.; Zhuang, H.-Z. *J. Colloid Interface Sci.* **1995**, *176*, 277.
(8) Chen, X.; Lee, H. F.; Gardella, J. A., Jr. *Macromolecules* **1993**, *26*, 4601.
(9) Chen, X.; Gardella, J. A., Jr.; Kumler, P. L. *Macromolecules* **1993**, *26*, 3778.
(10) Chen, X.; Gardella, J. A., Jr. *Macromolecules* **1994**, *27*, 3363.
(11) Chen, X.; Gardella, J. A., Jr.; Ho, T.; Wynne, K. J. *Macromolecules* **1995**, *28*, 1635.
(12) Dwight, D. W.; McGrath, J. E.; Riffle, J. S.; Smith, S. D.; York, G. A. *J. Electron Spectrosc.* **1990**, *52*, 457.
(13) LeGrand, D. G.; Gaines, G. L. *Polym. Prepr. Am. Chem. Soc.* **1970**, *11*, 442.
(14) Gaines, G. L.; Bender, G. W. *Macromolecules* **1972**, *5*, 82.
(15) Gaines, G. L. *Macromolecules* **1979**, *12*, 1011.
(16) Chen, J.-X.; Gardella, J. A., Jr. *PMSE Prepr. Am. Chem. Soc.* **1994**, *71*, 447.
(17) Chen, J.-X.; Gardella, J. A., Jr. *PMSE Prepr. Am. Chem. Soc.* **1996**, *75*, 404.
(18) Schmidt, J. J.; Gardella, J. A., Jr.; Salvati, L., Jr. *Macromolecules* **1989**, *22*, 4489.
(19) Chen, J.-X.; Zhuang, H.-Z.; Gardella, J. A., Jr. *Crit. Rev. Surf. Chem.*, Submitted.
(20) Harrick, N. J. *Internal Reflection Spectroscopy*; John Wiley & Sons: New York, 1979.
(21) Mirabella, F.; Harrick, N. J. *Internal Reflection Spectroscopy: Review and Supplement*; Harrick Scientific: Ossining, NY, 1985.
(22) Chen, J.-X.; Gardella, J. A., Jr. *Appl. Spectrosc.*, in press.
(23) Vargo, T. G.; Gardella, J. A., Jr. *J. Vac. Sci. Technol.* **1989**, *A7*, 1733.
(24) Zhuang, H.-Z.; Gardella, J. A., Jr. *Macromolecules* **1997**, *30*, 3632.
(25) Schmitt, R. L.; Gardella, J. A., Jr.; Chin, R. L.; Magill, J. H.; Salvati, L., Jr. *Macromolecules* **1985**, *18*, 2675.
(26) Xia, D.; Proctor, A.; Hercules, D. M. *Macromolecules* **1997**, *30*, 63.
(27) *CRC Handbook of Polymer−Liquid Interaction Parameters and Solubility Parameters*; Barton, A. F. M., Ed.; CRC: Boston, 1990.
(28) Ballistreri, A.; Garozzo, D.; Montaudo, G. *Macromolecules* **1984**, *17*, 1312.
(29) Bletsos, I. V.; Hercules, D. M.; vanLeyen, D.; Benninghoven, A. *Macromolecules* **1987**, *20*, 407.
(30) Selby, C. E.; Stuart, J. O.; Clarson, S. J.; Smith, S. D.; Sabata, A.; van Ooij, W. J.; Cave, N. G. *J. Inorg. Organomet. Polym.* **1994**, *4*, 85.
(31) Clarson, S. J.; Stuart, J. O.; Selby, C. E.; Sabata, A.; Smith, S. D.; Ashraf, A. *Macromolecules* **1995**, *28*, 674.
(32) *CRC Handbook of Chemistry and Physics*, 73rd ed.; Lide, D. R., Ed.; CRC: Boca Raton, FL, 1992.
(33) Weng, L. T.; Bertrand, P. *Surf. Interface Anal.* **1995**, *23*, 879.
(34) Ekgasit, S.; Ishida, H. *Appl. Spectrosc.* **1996**, *50*, 1187.

MA980639B